Journal of Geoscience and Environment Protection, 2026, 14(2), 19-35
https://www.scirp.org/journal/gep
ISSN Online: 2327-4344
ISSN Print: 2327-4336

Spatiotemporal Variability and Dominant Modes of Temperature Extremes over Africa during 1979-2024

Baraka Charles Bunini[1], Yi Fan[1*], Elisia Hamisi Zobanya[1,2]

[1]State Key Laboratory of Climate System Prediction and Risk Management/Key Laboratory of Meteorological Disaster, Ministry of Education/Collaborative Innovation Center on Forecast and Evaluation of Meteorological Disasters/School of Atmospheric Science, Nanjing University of Information Science and Technology, Nanjing, China
[2]Tanzania Meteorological Authority (TMA), Forecasting office Central Zone, Dodoma, Tanzania
Email: *fanyi@nuist.edu.cn

How to cite this paper: Bunini, B. C., Fan, Y., & Zobanya, E. H. (2026). Spatiotemporal Variability and Dominant Modes of Temperature Extremes over Africa during 1979-2024. *Journal of Geoscience and Environment Protection, 14,* 19-35.
https://doi.org/10.4236/gep.2026.142002

Received: December 24, 2025
Accepted: January 31, 2026
Published: February 3, 2026

Abstract

Temperature extremes are intensifying globally due to anthropogenic climate change, with Africa emerging as a hotspot of vulnerability despite contributing minimally to global emissions. Therefore, in this study we investigate the spatial and temporal variability of eight ETCCDI-based indices (TX90p, TN90p, TX10p, TN10p, TXx, TNx, TXn and TNn) over Africa during the period 1979-2024 using ERA5 reanalysis data. Empirical Orthogonal Function (EOF) analysis was applied to extract dominant modes of variability, and North test was used to assess the significance of each mode as well as we assessed the trend through 11-year moving average and standard deviation. Results show that the first EOF modes of warm-related indices such as TX90p, TN90p, TXx and TNx exhibit strong continent-wide warming patterns, while cold-related indices such as TX10p, TN10p, TNn, and TXn reveal declining cold extremes with more localized spatial signals. Temporal analysis of detrended principal components using 11-year moving averages and standard deviations highlights increasing trends and variability in warm extremes, particularly since the early 2000s, and a simultaneous reduction in cold extremes and their interannual fluctuations. Statistical testing (Mann-Kendall, $p < 0.05$) confirms the significance of several of these trends, reinforcing the robustness of the observed changes. These findings underscore the growing climate risks associated with extreme temperatures in Africa and provide valuable insights for regional adaptation strategies, early warning system, and climate resilience planning.

Keywords

Temperature Extreme, Africa, Warming, Increasing Trends

1. Introduction

Temperature extremes have intensified globally due to anthropogenic climate change, affecting ecosystems, health, energy demand, and food security (IPCC, 2023). Over recent decades, both the frequency and intensity of warm extremes have increased, while cold extremes have declined globally (Seneviratne et al., 2014). Human-induced warming often manifests its most damaging effects through extreme weather and climate events, particularly temperature extremes. Among these, heat waves are recognized as some of the deadliest natural hazards. The increasing frequency and severity of heat wave events have been linked to rising human mortality and widespread agricultural losses. These events carry substantial socioeconomic consequences, disrupting sectors such as agriculture, infrastructure, and energy production and consumption. Heat waves significantly threaten public health by increasing illness and mortality rates, especially among vulnerable populations. Between 1999 and 2009, California recorded 11,000 additional hospital admissions due to extreme heat. The European heat wave in 2003 resulted in up to 70,000 deaths. In 2015, severe heat in India and Pakistan led to approximately 2500 and 700 deaths, respectively. Similarly, Russia's 2010 heat wave caused nearly 15,000 deaths and an estimated economic loss of about 15 billion USD (Engdaw et al., 2022).

Although Africa contributes relatively little to global greenhouse gas emissions, it remains one of the regions most severely affected by climate-related extremes (Mahlstein et al., 2011). The continent is situated in a climatic zone where the signal of temperature change is projected to emerge earlier than in many other parts of the world, increasing its vulnerability to climate variability. Observational studies have reported significant warming trends and an increase in heatwaves across several African subregions, including the Sahel, West Africa, and parts of Southern Africa (Engelbrecht et al., 2015; New et al., 2006). As global warming intensifies, temperature extremes are projected to become more frequent and severe across the continent. North Africa is expected to experience the most pronounced warming, whereas East Africa is projected to undergo relatively smaller temperature increases between the 1.5˚C and 2˚C warming thresholds. The frequency and severity of extreme heat events are also projected to rise, especially in North Africa. However, limiting global warming to 1.5˚C could significantly reduce the intensity and occurrence of these extreme events, with North Africa gaining the most benefit compared to tropical regions (Nangombe et al., 2019; Pearce et al., 2014).

Temperature extremes serve as vital indicators of climate change and its potential impact on societies and ecosystems. Commonly used indices such as the annual maximum of daily maximum temperature (TXx), annual minimum of daily minimum temperature (TNn), frequency of warm days (TX90p), and frequency of cold nights (TN10p) are widely adopted for assessing the intensity, duration, and frequency of temperature extremes. These standardized indices, developed under international guidelines, allow for consistent analysis across regions and

time periods (Seneviratne et al., 2014; Zhang et al., 2011). In the African context, application of these indices has consistently revealed increasing trends in warm extremes (example TXx, TX90p, TN90p) and a decline in cold extremes (example TX10p, TN10p) (Diba et al., 2022; Dosio et al., 2018; Moron et al., 2016). This emerging pattern signifies an overall shift toward warmer climate conditions, carrying profound implications for public health, agricultural productivity, and water resource management across the continent.

However, the spatial coherence and dominant patterns of temperature extremes across the continent remain understudied (Collins, 2011). This study addresses that gap by analyzing the spatial and temporal characteristics of eight ETCCDI-based temperature extreme indices over Africa. The analysis is conducted in two parts; spatial and Temporal Patterns via EOF Analysis in which annual fields of each index were subjected to Empirical Orthogonal Function (EOF) to extract dominant modes of variability, with the North test applied to confirm the statistical separation between leading modes (North, 1982) and Trend Analysis and Long-Term Variability where the resulting principal components (PC1 and PC2) were detrended and used to calculate 11-year moving averages and standard deviations, capturing long-term trends and interdecadal variability. This combined approach enhances understanding of where and how temperature extremes are changing across Africa. By linking spatial patterns with temporal dynamics, this study provides critical insight into the evolving nature of climate extremes, offering a basic for future risk assessment, adaptation planning, and climate resilience strategies across the different Africa regions.

2. Data and Methodology

2.1. Data

The present study utilizes ERA5 reanalysis daily maximum and minimum temperature data from the European Centre for Medium-Range Weather Forecasts (ECMWF) (Hersbach et al., 2020).The dataset covers a 46-years period (1979-2024) over the Africa region, bounded between 20˚W to 55˚E longitude and 35˚S to 40˚N, with a high spatial resolution of $0.25^{\circ}\times0.25^{\circ}$. The data sets are publicly available and can be accessed through the Copernicus Climate Data Store at: https://cds.climate.copernicus.eu/datasets/derived-era5-single-levels-daily-statistics?tab=download.

2.2. Temperature Extreme Indices

Following the definitions established by the Expert Team on Climate Change Detection and Indices (ETCCDI) as outlined by Zhang et al. (2011), this study computed eight extreme temperature indices. A description of these indices is provided in **Table 1** (Yin & Sun, 2018).

2.3. Empirical Orthogonal Function (EOF) Analysis

Empirical Orthogonal Function (EOF) analysis was applied to identify the dominant

Table 1. Definition of Extreme Temperature indices used in this study

Extreme indices	Indicator name	Definition	Unit
TXx	Max T_{max}	Annual maximum value of daily maximum temperature	˚C
TXn	Min T_{max}	Annual minimum daily maximum temperature	˚C
TNn	Min T_{min}	Annual minimum value of daily minimum temperature	˚C
TNx	Max T_{min}	Annual maximum value of daily minimum temperature	˚C
TX90p	Warm days	Days when TXx > 90^{th} percentile	%
TX10p	Cold days	Days when TXx < 10^{th} percentile	%
TN10p	Cold night	Days when TNx < 10^{th} percentile	%
TN90p	Warm night	Days when TNx > 90^{th} percentile	%

spatial patterns of temperature extremes and their temporal evolution across Africa (Fan et al., 2022; Hannachi et al., 2007). The analysis was conducted annually for each temperature index, extracting the first two leading EOF modes. The North test was employed to assess the statistical significance and separation between the modes. Typically, EOF1 captures the most dominant spatial structure, highlighting key hotspot regions. The corresponding principal component (PC) time series illustrates the temporal variability associated with these spatial patterns, providing insights into how temperature extremes have evolved over time.

2.4. Trend Analysis

To assess long-term trends and interdecadal variability in temperature extremes, this study applied an 11-year moving average and moving standard deviation to the principal components (PCs) derived from the EOF analysis (Pearce et al., 2014). Detrending was applied to the principal components (PCs) as part of the preprocessing step. The detrended PCs were then used for both the 11-year moving average and 11-year moving standard deviation calculations. This approach was applied to each of the eight extreme temperature indices, providing insights into the evolving behavior of extreme temperature patterns across Africa and highlighting periods of intensified or reduced variability. To evaluate the statistical significance of trends in both 11-year moving average and standard deviation the Mann-Kendall trend test was applied at the 95% confidence level ($p < 0.05$).

3. Results and Discussion

3.1. Spatial and Temporal Distribution of Temperature Extremes Indices over Africa

Figure 1 Shows the first two leading empirical orthogonal function (EOF) modes and their corresponding principal component (PCs) time series for the TX90p and

TN90p indices over Africa from 1979 to 2024. The first EOF mode (EOF1) accounts for a substantial proportion of the total variance, 60.3% for TX90p (**Figure 1(a)**) and 65.1% for TN90p (**Figure 1(e)**), indicating a dominant and spatial coherent pattern of increasing warm days and warm nights across much of the continent. These modes highlight widespread intensification of temperature extremes, particularly the central and other parts of Africa. The corresponding PC1 time series (**Figure 1(b)** and **Figure 1(f)**) reveal a consistent upward trend over the study period, suggesting a robust increase in the frequency of extremely warm days and nights. These observed trends align with the previous study by Odunmorayo et al. (2025a), who identified the intensification of temperature extremes (TX90p and TN90p) in Africa. The second EOF modes (EOF2), explain 6.7% (TX90p) and 6.5% (TN90p) of the variance (**Figure 1(c)** and **Figure 1(g)**), capture more localized variability. For TX90p, the pattern emphasizes stronger warm signals over southern Africa, while TN90p shows enhanced signals over both northern and southern subregions. The PC2 time series for both indices (**Figure 1(d)** and **Figure 1(h)**) exhibit slight downward trends, it is possible that it could reflect changes in regional circulation patterns or land-atmosphere feedback, which influence localized heat extremes (Kroll et al., 2025; Uckan et al., 2025).

Figure 2 illustrates the spatial and temporal characteristics of the first two Empirical Orthogonal Function (EOF) modes for TX10p and TN10p indices over

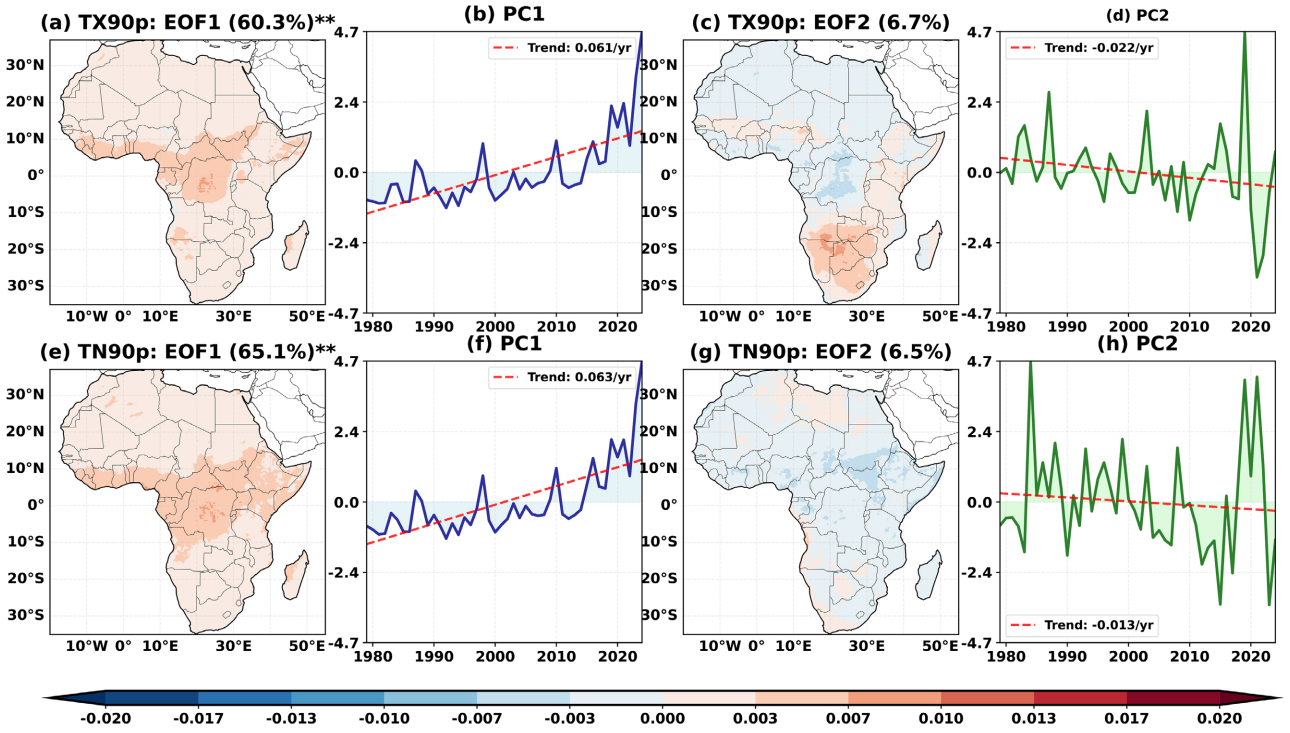

Figure 1. Spatial and temporal pattern of TX90p and TN90p indices over Africa for the period 1979 to 2024 Panels (a)-(c) and (e)-(g) show the first two EOFs spatial modes of TX90p and TN90p indices respectively, representing the dominant pattern of variability. Panels (b)-(d) and (f)-(h) show the corresponding principal components time series of TX90p and TN90p indices respectively, indicating the temporal evolution of these patterns. The two asterisks (**) indicate the modes are significantly separated according to North test.

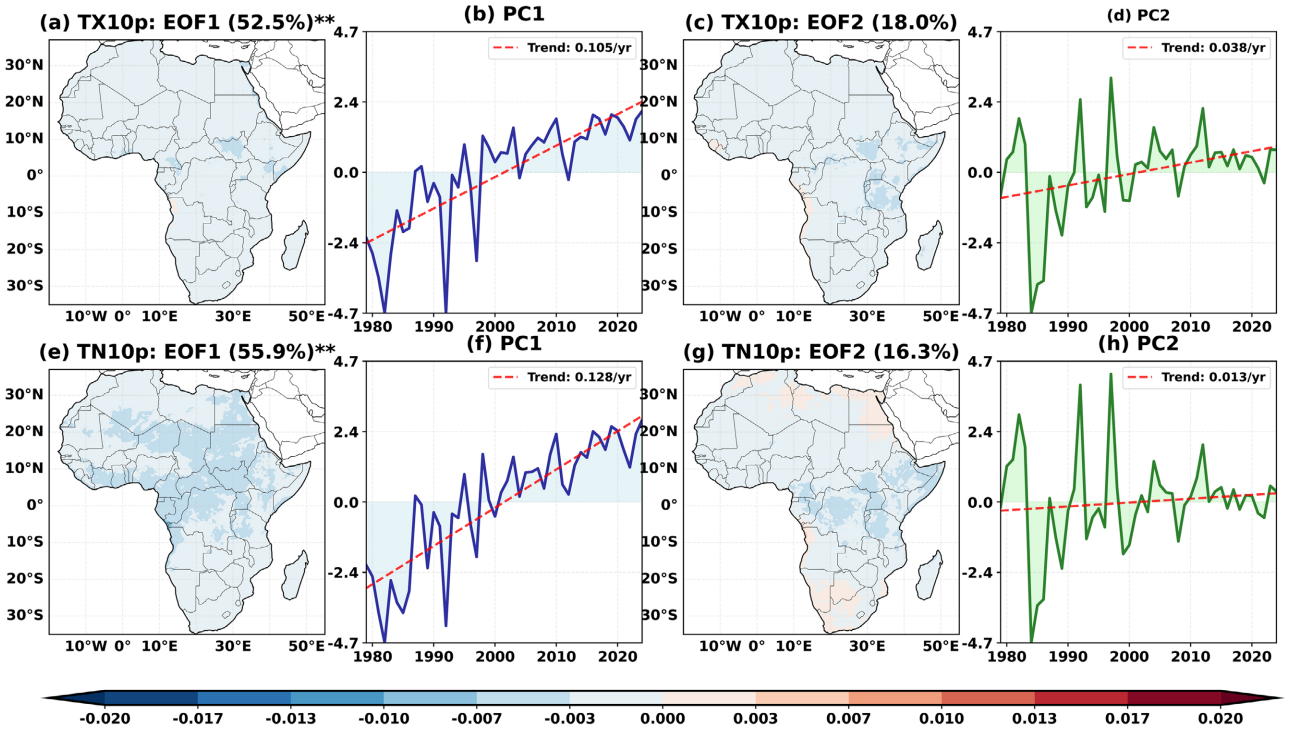

Figure 2. Same as in **Figure 1**, but for TX10p and TN10p indices.

Africa. The leading modes (EOF1), shown in panels 2a and 2e, explain 52.5% and 55.9% of the total variance, respectively, indicating a dominant continent-wide pattern characterized by a decline in cold days and cold nights. The corresponding PC1 time series (**Figure 2(b)** and **Figure 2(f)**) reveal a consistent upward trend, suggesting a significant reduction in the frequency of cold extremes over the study period. These results are consistent with previous studies across Africa regions that reported similar warming trends and a decrease in cold events (Iyakaremye et al., 2021; Ogolo et al., 2024). The second EOF modes (**Figure 2(c)** and **Figure 2(g)**) explain 18.0% of the variance for TX10p and 16.3% for TN10p, capturing more localized variability. EOF2 for TN10p highlights weak positive signals over parts of northern and south Africa. The associated PC2 time series (**Figure 2(d)** and **Figure 2(h)**) show a slight upward trend, which may indicate regional warming hotspots or shifting frequencies of cold events. These findings align with those of van der Walt & Fitchett, (2021) and Gebrechorkos et al. (2019), who emphasized the regional nature of cold extremes and their gradual decline.

Figure 3 presents the leading EOF modes and corresponding principal components for TNn and TXn indices over Africa during the period 1979 to 2024. The first EOF modes (**Figure 3(a)** and **Figure 3(e)**) explain 20.1% and 22.5% of the total variance for TNn and TXn, respectively. Both modes show dominant negative anomalies, particularly over northern and western Africa, indicating a widespread decline in annual minimum temperatures (TNn) and annual minimum of daily maximum temperatures (TXn). These negative signals suggest an ongoing reduction in the frequency and intensity of cold extremes across these regions.

However, for TXn, there are weak positive anomalies over central to southern Africa, suggesting localized warming trends where extreme cold days are becoming less frequent. The associated PC1 time series (Figure 3(b) and Figure 3(f)) display statistically significant negative linear trends, reinforcing the overall warming pattern and the decline in cold extremes across much of the continent. The second EOF modes (Figure 3(c) and Figure 3(g)) capture more localized and spatially contrasting patterns. For TNn (Figure 3(c)), a dipole-like structure emerges, with negative anomalies over northern Africa and positive signals over western and southern parts. In contrast, the TXn second mode (Figure 3(g)) shows strong positive signals concentrated over northern Africa, indicating possible localized cooling persistence. These contrasting spatial patterns may reflect the influence of regional climate dynamics. The PC2 time series (Figure 3(d) and Figure 3(h)) show mixed behavior: TNn exhibits a downward trend, while TXn shows a slight upward trend, suggesting regional disparities in cold extreme evolution. These results emphasize the complex and heterogeneous nature of temperature extremes across Africa, where both large-scale warming and localized variability coexist.

The first modes of variability account for 26.5% and 32.9% of the total variance for TXx and TNx, respectively, as illustrated in Figure 4(a) and Figure 4(e). These EOF1 patterns reveal a broad, continent wide positive pattern, indicating a substantial and spatially coherent intensification of warm extremes across most regions of Africa. This suggests that both the annual maximum of daily maximum temperature (TXx) and the annual maximum of daily minimum temperature (TNx) have been increasing consistently over time. In contrast, the second EOF

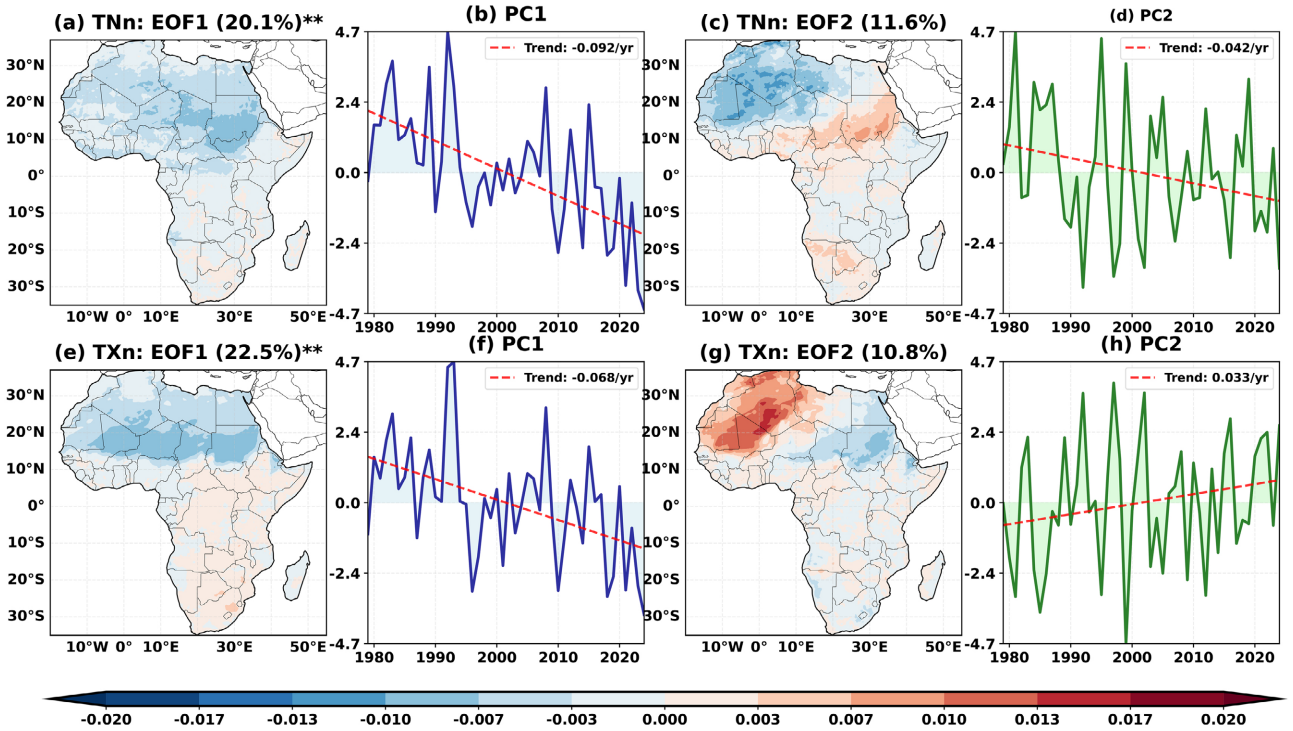

Figure 3. Same as in Figure 1, but for TNn and TXn indices.

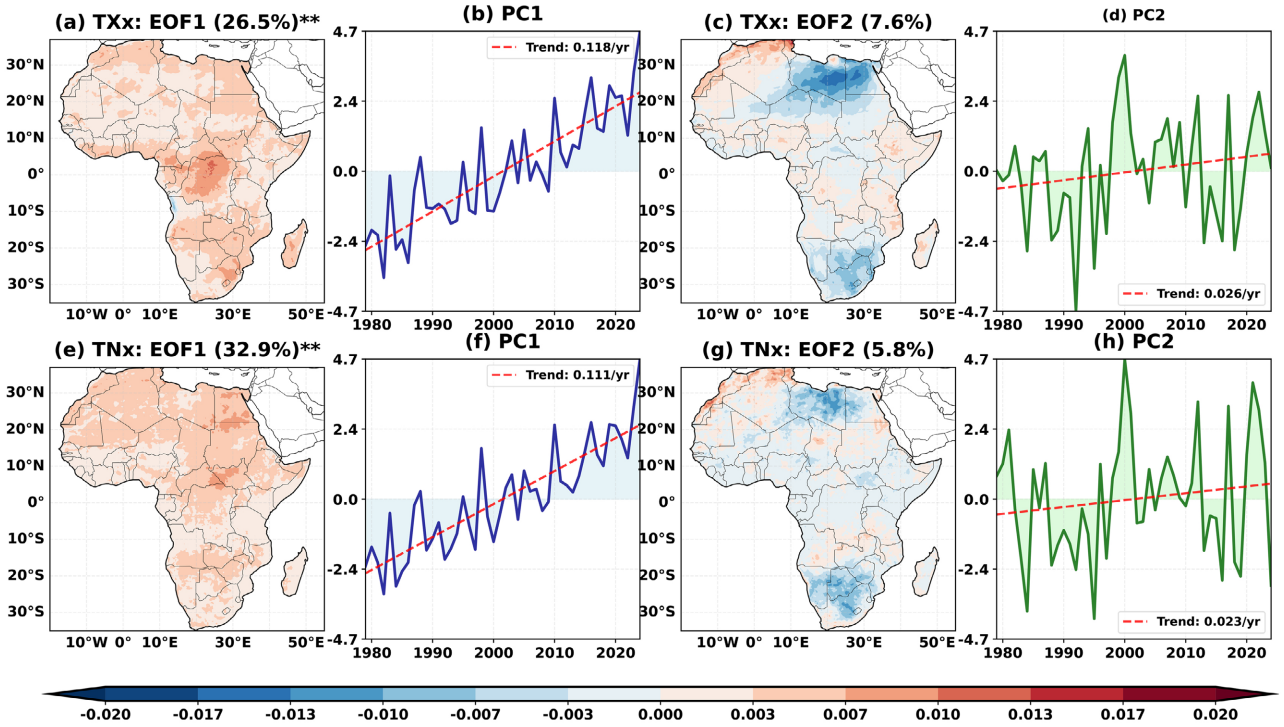

Figure 4. Same as in **Figure 1**, but for TXx and TNx indices.

modes (**Figure 4(c)** and **Figure 4(g)**) display more regional variability, with negative anomalies particularly over parts of northern and southern Africa. These patterns may reflect regional contrasts in warming rates or local influences such as topography, land-use change, or circulation features affecting extreme temperature. The associated principal components (PC1 and PC2 for both indices; **Figure 4(b)**, **Figure 4(d)**, **Figure 4(f)**, and **Figure 4(h)**) show statistically significant increasing trends throughout the study period, further confirming the widespread intensification of warm temperature extremes across the continent. These trends indicate that extreme heat events, both daytime and night-time, are becoming more frequent and intense across Africa.

3.2. Trend Analysis of Temperature Extremes Indices over Africa

In this analysis, we examined the temporal evolution of warm temperature extremes over Africa using 11-year moving averages and standard deviations of the detrended principal components (PCs) derived from EOF analysis. Our focus was on the TX90p (warm days) and TN90p (warm nights) indices between 1979 to 2024. As shown in **Figure 5**, we found that the first principal components (PC1) for both indices (panels a and e in **Figure 5**) exhibit a notable negative trend in the moving average up to the early 2000s, followed by a sharp positive shift. This trend suggests that warm extremes were relatively less frequent in earlier decades but have increased markedly in the last two decades. The decreasing trends in the 11-year moving averages of TX90p and TN90p PC1 were found to be statistically significance ($p < 0.05$), confirming a real shift in the mean state. In contrast, it

was observed that the PC2 moving averages (Panels c and g in Figure 5) remained relatively stable throughout the study period, with near-zero linear trends, indicating less contribution to long-term shifts. On the other hand, the 11-year moving standard deviations (Panels b, d, f, and h in Figure 5) reveal an increasing trend in variability, particularly after the early 2000s. The increases in variability were statistically significant for both TX90p and TN90p PC1 and PC2 indicating stronger fluctuations in the occurrence of warm days and nights. For instance, we found that the TX90p PC2 standard deviation shows a strong positive trend (0.0333), highlighting a rise in interannual fluctuations. This growing variability points to more irregular and widespread occurrences of extremely warm days and nights. These findings are consistent with observed and projected climate patterns in Africa, where warming has accelerated in recent decades (Malik et al., 2024). The amplification of both mean values and variability of warm extremes aligns with warming trends and supports concerns about increased climate risk across African regions. Notably, the Sahel, parts of southern Africa, and northern subregions have shown heightened sensitivity to heat extremes (Odunmorayo et al., 2025b).

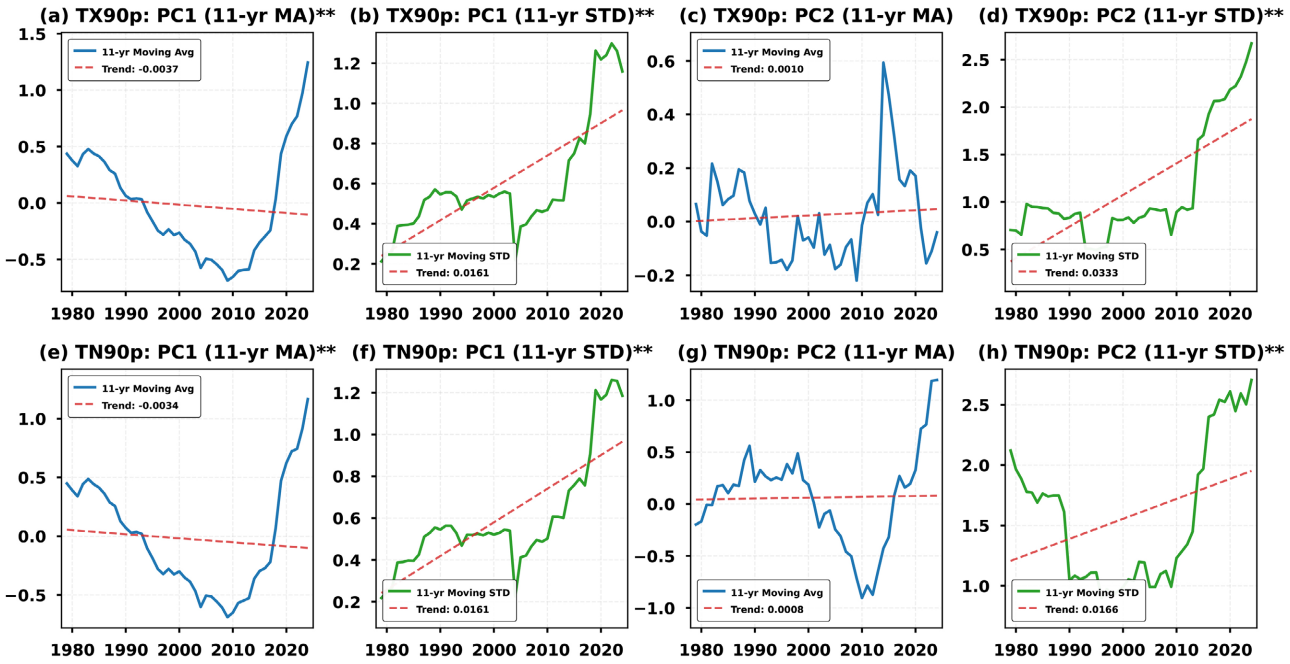

Figure 5. Trend analysis of TX90p and TN90p indices over Africa (1979-2024). Panels (a)-(c) and (e)-(g) shows 11-year moving average of the detrended PCs series of TX90p and TN90p indices. Panels (b)-(d) and (f)-(h) show 11-year moving standard deviation of the detrended PCs series of TX90p and TN90p indices. The two asterisks (**) indicate the significant at the 95% confidence level ($p < 0.05$).

The analysis of cold-related temperature indices, specifically TX10p (cold days) and TN10p (cold nights), is shown in Figure 6, reveal relatively stable long-term behavior in their mean occurrence across Africa over the study period. The 11-year moving averages of the first and second principal components (PC1 and PC2)

Panels (a, c, e and g in Figure 6) show linear trends that are near-zero or only slightly positive for example, a trend of 0.0001 for TX10p PC1 and 0.0048 for TN10p PC2 indicating that, on average, the frequency of cold extremes has remained relatively constant. These near-zero trends were not statistically significant, supporting the conclusion that the central tendency of cold extremes has not experienced major long-term changes. These results suggest an absence of strong long-term warming or cooling signals in the central tendency of cold extremes, though some interdecadal fluctuations are evident. However, panels (b, d, f and h in Figure 6) the 11-year moving standard deviations show a different trend. Across both indices and leading modes, a consistent and significant downward trend is observed for instance, −0.0259 for TX10p PC1 and −0.0581 for TN10p PC2 particularly intensifying after the early 2000s. This decline in variability implies that the year-to-year fluctuations in the frequency of cold days and nights have become less pronounced. One possible explanation is that warming trends across the continent have led to fewer extremely cold events and a narrowing of the distribution of daily temperature. Reduced variability could also be linked to changes in circulation patterns, such as weaker cold air intrusions or shifts in regional atmospheric dynamics. While the overall occurrence of cold extremes has not dramatically decreased, the significant reduction in variability indicates a more consistent climate state with respect to cold extremes, suggesting a climate system gradually stabilizing toward fewer cold anomalies.

The temporal behavior of the coldest temperature extremes, represented by the TNn (coldest nights) and TXn (coldest days) indices, demonstrates a relatively stable mean frequency across Africa during the study period. As illustrated in Figure 7, panels (a), (c), (e), and (g), the 11-year moving averages of PC1 and

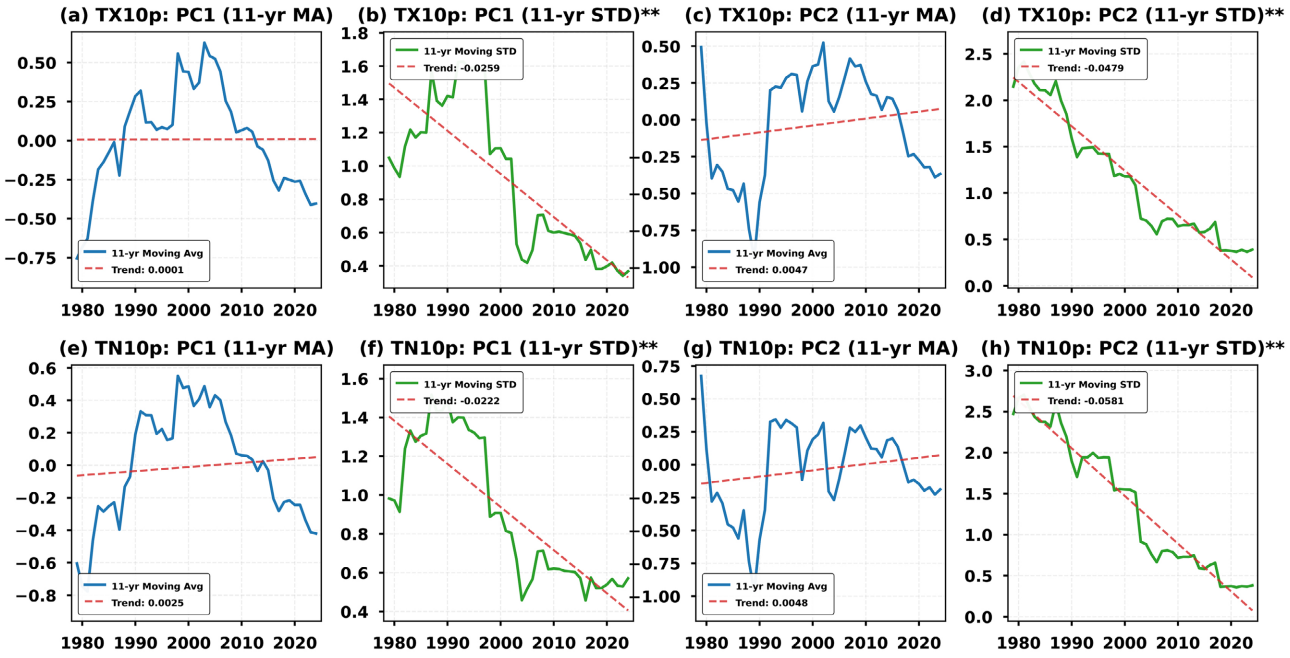

Figure 6. Same as in Figure 5, but for TX10p and TN10p indices.

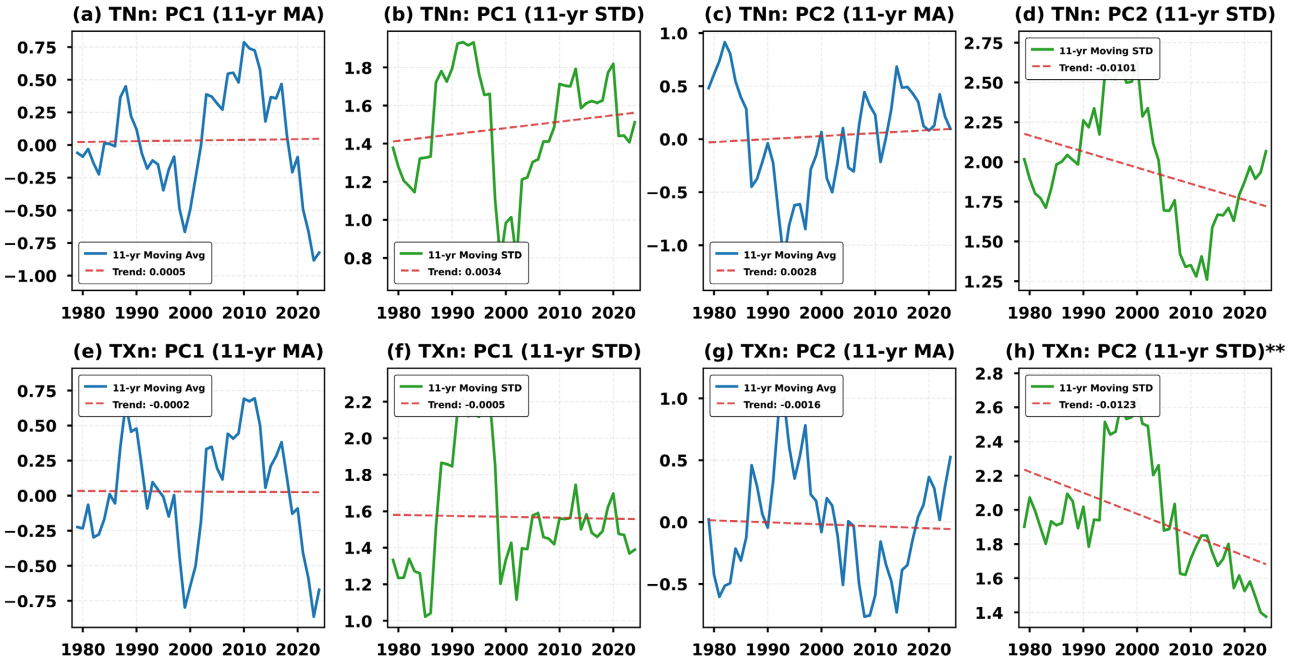

Figure 7. Same as in **Figure 5**, but for TNn and TXn indices.

PC2 for both indices show nearly flat or slightly positive linear trends for example, a trend of 0.0005 in TNn PC1 and -0.0016 in TXn PC2 indicating no strong long-term change in the average occurrence of coldest extremes. These trends were not statistically significant ($p < 0.05$), confirming the absence of a dominant long-term warming or cooling signal in the mean state of coldest days and nights. This stability could be due to regional climate mechanisms, such as stable circulation patterns or the moderating effects of altitude and land atmosphere feedback in certain regions. Meanwhile, the 11-year moving standard deviations, shown in **Figure 7**, panels (b), (d), (f), and (h), reveal mixed trends in interannual variability. For instance, PC1 STD for TNn shows a slight increasing trend (0.0034), but it was not statistically significant. In contrast, PC2 STD for TXn exhibits a significance decline (−0.0123). Other components like PC2 STD for TNn (−0.0101) and PC1 STD for TXn (−0.0005) also indicate modest decreases, but these were not significant. This trend suggests that while the average frequency of cold extremes remains largely unchanged, their variability is gradually decreasing in some regions. The decline in standard deviation could reflect a reduced range of cold anomalies, potentially linked to a warming baseline climate that suppresses extreme cold intrusions. These findings emphasize the spatial and temporal complexity of cold extremes in Africa, where the impact may be more evident in variability than in the frequency of occurrences.

The temporal evolution of annual extreme temperature indices TXx (hottest day) and TNx (hottest night) over Africa from 1979 to 2024 reveals insights into long-term changes in temperature extremes. As shown in **Figure 8**, panels (a), (c), (e), and (g), the 11-year moving averages of PC1 and PC2 for both indices exhibit generally stable or slightly negative trends for example, −0.0012 for TXx

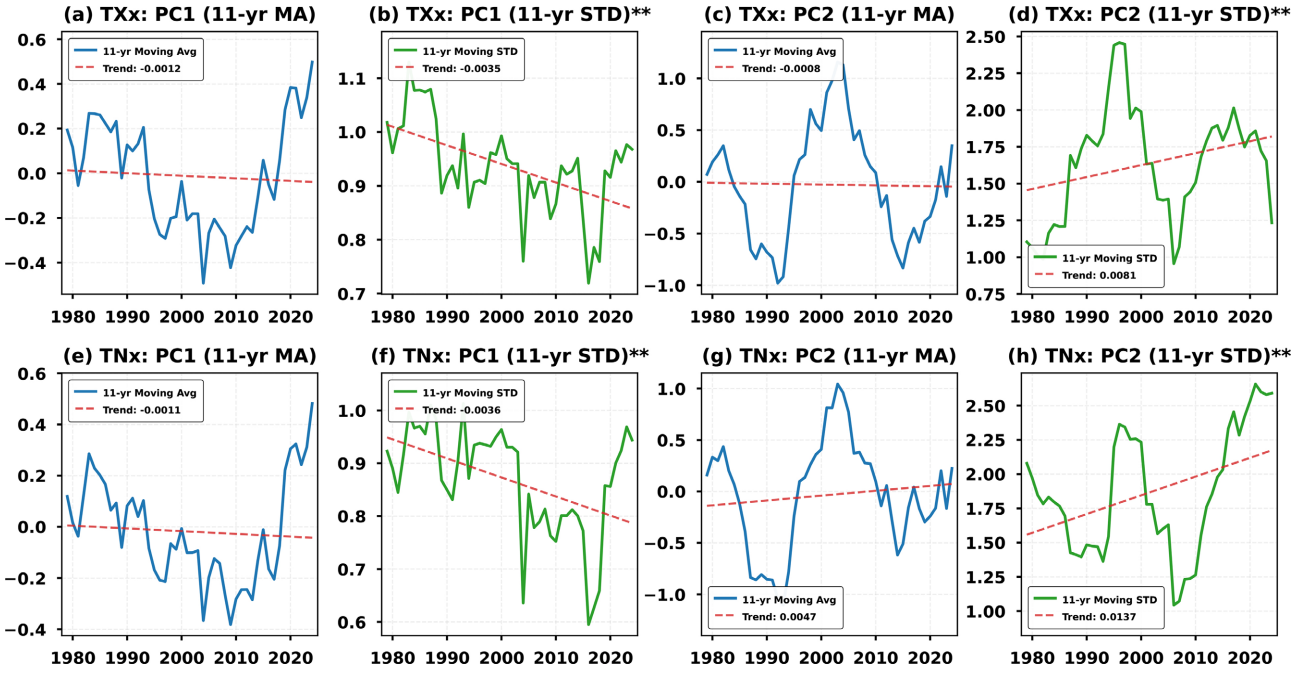

Figure 8. Same as in **Figure 5**, but for TXx and TNx indices.

PC1 and −0.0011 for TNx PC1. These trends were not statistically significant, indicating that at the continental scale, the mean amplitude of the hottest day and night temperatures has not significantly changed over the analysis period. The presence of fluctuations without a strong trend indicates interdecadal variability, possibly influenced by multi-decadal climate oscillations or internal atmospheric dynamics, rather than a persistent warming trend in annual extremes for these modes. In contrast, the 11-year moving standard deviations, shown in panels (b), (d), (f), and (h) in **Figure 8**, indicate more dynamic behavior. The PC1 STD trends for TXx and TNx show slight decreases (−0.0035 and −0.0036, respectively), and both were statistically significant, pointing to reduced variability in some dominant modes. However, PC2 STD for TXx and TNx shows notable positive trends with statistically significant increases, particularly 0.0081 for TXx PC2 and 0.0137 for TNx PC2, with the steepest increase occurring after the early 2000s. This rise in variability for the secondary modes may reflect increasing regional disparities in extreme heat events where some localized areas experience sharper or more erratic increases in annual maximum temperature. These results imply that although the continent-wide averages of hottest extremes appear stable, the spatial structure and variability of these events have evolved, potentially driven by regional climate feedback, land surface changes, or warming-induced alterations in atmospheric circulation.

3.3. Discussion

This study examined the dominant spatial patterns, long-term trends, and temporal variability of eight ETCCDI temperature extreme indices across Africa (1979-2024), integrating empirical orthogonal function (EOF) analysis with trend

analysis using 11-year moving average and standard deviation. The findings reveal robust warming signals and evolving patterns of temperature extremes across the continent, with distinct behaviors between warm and cold indices, pointing to both large-scale warming and regional variability.

The leading EOF modes of warm indices such as TX90p and TN90p explain a substantial proportion of total variance (60.3% and 65.1%, respectively in **Figure 1(a)** and **Figure 1(e)**), revealing continent-wide patterns of intensifying warm days and nights. The higher explained variance underscores a coherent warming mode that transcends regional boundaries and confirms that warm extremes are a pervasive feature of Africa's climate. These pattern patterns align with global assessments showing increases in warm extreme under warming climates (Seneviratne et al., 2014) (Zhang et al., 2011). The associated principal component (PC1) time series shows clear upward trends, especially early 2000s, indicating that the frequency of extreme warming events has increased significantly in recent decades. Additionally, the standard deviation trends of PC1 and PC2 for TX90p and TN90p revealed significant increases, highlighting growing interannual variability in warm extremes. This asymmetry between increasing warm extremes and decreasing cold extremes provides further evidence that the temperature distribution is becoming skewed, rather than responding symmetrically to climate warming. In contrast, cold indices such as TX10p, TN10p, TNn, and TXn (in **Figure 2** and **Figure 3**) revealed more muted spatial modes in EOF1, with lower variance explained compared to warm indices. The spatial structure suggests that cold extremes are less coherent across the continent, which resonates with findings that warming trends tend to be stronger in warm extremes, while cold extremes show greater spatial heterogeneity. However, the decrease in the intensity and frequency of cold extremes as indicated by negative trends in the principal components (shown in TNn and TXn in **Figure 3**) confirms that cold events are becoming less frequent and less intense. Yet, this does not reflect a purely symmetric response. The significant decrease in standard deviation of cold indices (example TN10p PC2 STD) suggests a narrowing of distribution on the cold side, supporting an asymmetric shift. This trend implies that warming disproportionately reduces cold extremes, consistent with studies that highlight skewed warming effects (Donat et al., 2013)

In long-term trends cold indices show relatively stable long-term moving averages, indicating little change in mean conditions, but the moving standard deviations reveal statistically significant decreasing variability in some modes. For example, indices like TN10p in **Figure 6(f)** and **Figure 6(h)** show a strong and significant downward trend in variability after the early 2000s, this implies that cold extremes occur less sporadically over time. This decreasing variability may reflect both a reduction in the range of cold anomalies and the influence of warming, which compresses the lower tail of the temperature distribution. The mixed trends observed in TXn and TNn STDs (**Figure 7(b)**, **Figure 7(d)**, **Figure 7(f)** and **Figure 7(h)**) further highlight that cold extremes are influenced by a complex interplay

of regional circulation patterns and localized climate feedback.

While continent-wide warming is evident, the spatial patterns from EOF2 and PC2 time series reveal important regional contrasts. Warm indices show positive in secondary modes over southern parts and central Africa (**Figure 3(c)** and **Figure 3(g)**), suggesting that some regions have experienced stronger increases in heat extremes due to localized climate feedback or regional teleconnections. For cold indices, dipole pattern in EOF2 (**Figure 3(c)**) indicate spatial heterogeneity negative anomalies in northern Africa contrasting with positive anomalies in southern regions highlighting how different subregions respond differently to the same climate forcing or changing. These regional differences can be attributed to variations in atmospheric circulation, land surface conditions and feedback mechanisms. For instance, change in the west African monsoon, the subtropical ridge, and the extent of the Sahara heat low can modulate temperature extreme in Weste and North Africa. Southern Africa's unique climate drivers, including the influence of Indian Ocean subtropical high and local soil moisture feedback, may explain the stronger warm signals in certain secondary modes. These spatial anomalies may reflect teleconnections associated with North Oscillation (NAO), Indian Ocean Dipole (IOD), or even Southern Annular Mode (SAM), which have been linked to seasonal variability in African temperatures (Hurrell & Deser, 2010). Therefore, attributing these patterns solely to regional dynamics may oversimplify their origin. These identified dipole signatures suggest that extratropical and ocean-atmosphere interactions contribute significantly to spatial heterogeneity in cold extremes.

4. Conclusion

In this study, we investigated the spatial and temporal characteristics of eight ETCCDI-based temperature extreme indices over Africa from 1979-2024, using Empirical Orthogonal Function (EOF) analysis and trend assessment through 11-year moving averages and standard deviations. The findings reveal a robust and continent-wide intensification of warm temperature extremes (TX90p, TN90p, TXx and TNx) and generally decline in cold extremes (TX10p, TN10p, TXn and TNn). The leading EOF modes highlighted coherent spatial patterns across Africa, particularly for warm indices, while secondary modes captured regional variability, reflecting localized climate dynamics. The increasing trends in warm indices as illustrated in principal components and the rising interannual variability especially since the early 2000s indicate growing climate stress on ecosystems and societies. Conversely, cold indices show relatively stable averages but declining variability, suggesting a reduction in both intensity and frequency of cold extremes. These trend patterns were further supported by statistical significance testing using Mann-Kendall method ($p < 0.05$), particularly the standard deviation of TX90p, TN90p, and cold indices showing statistically significant increasing and decreasing variability. This reinforces the robustness of the observed interannual changes.

These patterns emphasize the shifting nature of Africa climate extremes, influenced by regional climate drivers. The results contribute to a clear understanding of how, where, and at what rate temperature extremes are evolving across the continent. Despite the robust findings revealed in this study, further investigation is needed to better understand how larger-scale climate phenomena like ENSO, IOD, local atmospheric circulation, and land surface heat budget interact with regional warming patterns. Such analysis will be crucial for improving the anticipation and projection of future shifts in temperature extreme across Africa.

Acknowledgements

The authors acknowledge ECMWF for providing the ERA5 dataset and express gratitude to the Ministry of Commerce of China (MOFCOM) for supporting this research opportunity.

Conflicts of Interest

The authors declare no conflicts of interest regarding the publication of this paper.

References

Collins, J. M. (2011). Temperature Variability over Africa. *Journal of Climate, 24,* 3649-3666. https://doi.org/10.1175/2011jcli3753.1

Diba, I., Diedhiou, A., Famien, A. M., Camara, M., & Fotso-Nguemo, T. C. (2022). Changes in Compound Extremes of Rainfall and Temperature over West Africa Using CMIP5 Simulations. *Environmental Research Communications, 4,* Article 105003. https://doi.org/10.1088/2515-7620/ac9aa7

Donat, M. G., Alexander, L. V., Yang, H., Durre, I., Vose, R., Dunn, R. J. H. et al. (2013). Updated Analyses of Temperature and Precipitation Extreme Indices since the Beginning of the Twentieth Century: The HadEX2 Dataset. *Journal of Geophysical Research: Atmospheres, 118,* 2098-2118. https://doi.org/10.1002/jgrd.50150

Dosio, A., Mentaschi, L., Fischer, E. M., & Wyser, K. (2018). Extreme Heat Waves under 1.5 °C and 2 °C Global Warming. *Environmental Research Letters, 13,* Article 054006. https://doi.org/10.1088/1748-9326/aab827

Engdaw, M. M., Ballinger, A. P., Hegerl, G. C., & Steiner, A. K. (2022). Changes in Temperature and Heat Waves over Africa Using Observational and Reanalysis Data Sets. *International Journal of Climatology, 42,* 1165-1180. https://doi.org/10.1002/joc.7295

Engelbrecht, F., Adegoke, J., Bopape, M., Naidoo, M., Garland, R., Thatcher, M. et al. (2015). Projections of Rapidly Rising Surface Temperatures over Africa under Low Mitigation. *Environmental Research Letters, 10,* Article 085004. https://doi.org/10.1088/1748-9326/10/8/085004

Fan, Y., Li, J., Zhu, S., Li, H., & Zhou, B. (2022). Trends and Variabilities of Precipitation and Temperature Extremes over Southeast Asia during 1981-2017. *Meteorology and Atmospheric Physics, 134,* Article No. 78. https://doi.org/10.1007/s00703-022-00913-6

North, G. R., Bell, T. L., Cahalan, R. F., & Moeng, F. J. (1982). Sampling Errors in the Estimation of Empirical Orthogonal Functions. *Monthly Weather Review, 110,* 699-706. https://doi.org/10.1175/1520-0493(1982)110<0699:seiteo>2.0.co;2

Gebrechorkos, S. H., Hülsmann, S., & Bernhofer, C. (2019). Changes in Temperature and Precipitation Extremes in Ethiopia, Kenya, and Tanzania. *International Journal of Cli-*

matology, 39, 18-30. https://doi.org/10.1002/joc.5777

Hannachi, A., Jolliffe, I. T., & Stephenson, D. B. (2007). Empirical Orthogonal Functions and Related Techniques in Atmospheric Science: A Review. *International Journal of Climatology, 27,* 1119-1152. https://doi.org/10.1002/joc.1499

Hersbach, H., Bell, B., Berrisford, P., Hirahara, S., Horányi, A., Muñoz-Sabater, J. et al. (2020). The ERA5 Global Reanalysis. *Quarterly Journal of the Royal Meteorological Society, 146,* 1999-2049. https://doi.org/10.1002/qj.3803

Hurrell, J. W., & Deser, C. (2010). North Atlantic Climate Variability: The Role of the North Atlantic Oscillation. *Journal of Marine Systems, 79,* 231-244. https://doi.org/10.1016/j.jmarsys.2009.11.002

IPCC (2023). *Climate Change 2021—The Physical Science Basis.* Cambridge University Press.

Iyakaremye, V., Zeng, G., & Zhang, G. (2021). Changes in Extreme Temperature Events over Africa under 1.5 and 2.0°c Global Warming Scenarios. *International Journal of Climatology, 41,* 1506-1524. https://doi.org/10.1002/joc.6868

Kroll, J., Stephan, R., Feldman, A. F., Miralles, D. G., & Orth, R. (2025). *Increased Heating of the Land Surface as Hot-Dry Events Persist.* Preprint.

Mahlstein, I., Knutti, R., Solomon, S., & Portmann, R. W. (2011). Early Onset of Significant Local Warming in Low Latitude Countries. *Environmental Research Letters, 6,* Article 034009. https://doi.org/10.1088/1748-9326/6/3/034009

Malik, A., Stenchikov, G., Mostamandi, S., Parajuli, S., Lelieveld, J., Zittis, G. et al. (2024). Accelerated Historical and Future Warming in the Middle East and North Africa. *Journal of Geophysical Research: Atmospheres, 129,* e2024JD041625. https://doi.org/10.1029/2024jd041625

Moron, V., Oueslati, B., Pohl, B., Rome, S., & Janicot, S. (2016). Trends of Mean Temperatures and Warm Extremes in Northern Tropical Africa (1961-2014) from Observed and PPCA-Reconstructed Time Series. *Journal of Geophysical Research: Atmospheres, 121,* 5298-5319. https://doi.org/10.1002/2015jd024303

Nangombe, S. S., Zhou, T., Zhang, W., Zou, L., & Li, D. (2019). High-Temperature Extreme Events over Africa under 1.5 and 2 °C of Global Warming. *Journal of Geophysical Research: Atmospheres, 124,* 4413-4428. https://doi.org/10.1029/2018jd029747

New, M., Hewitson, B., Stephenson, D. B., Tsiga, A., Kruger, A., Manhique, A. et al. (2006). Evidence of Trends in Daily Climate Extremes over Southern and West Africa. *Journal of Geophysical Research: Atmospheres, 111,* D14. https://doi.org/10.1029/2005jd006289

Odunmorayo, M. T., Alani, B. O., & Adefisan, E. A. (2025b). Projected Change in Occurrence and Severity of Heatwaves over West Africa as Simulated by CMIP6 Models. *Journal of Disaster Science and Management, 1,* Article No. 16. https://doi.org/10.1007/s44367-025-00017-z

Odunmorayo, M. T., Arowolo, A. V., Okeyode, I. A., & Ebiendele, P. (2025a). Multi-Forcing Impacts on Temperature Extremes over Africa: Anthropogenic, Aerosols, Natural, and Solar Influences under Higher Emission Pathways. *Discover Atmosphere, 3,* Article No. 15. https://doi.org/10.1007/s44292-025-00043-9

Ogolo, E. O., Ojo, O. S., & Olabisi, I. O. (2024). Spatio-Temporal Distribution of Intensity and Frequency of Extreme Temperature Events over Nigeria. *Theoretical and Applied Climatology, 155,* 9961-9980. https://doi.org/10.1007/s00704-024-05215-y

Pearce, W., Holmberg, K., Hellsten, I., & Nerlich, B. (2014). Climate Change on Twitter: Topics, Communities and Conversations about the 2013 IPCC Working Group 1 Report. *PLOS ONE, 9,* e94785. https://doi.org/10.1371/journal.pone.0094785

Seneviratne, S. I., Donat, M. G., Mueller, B., & Alexander, L. V. (2014). No Pause in the Increase of Hot Temperature Extremes. *Nature Climate Change, 4,* 161-163. https://doi.org/10.1038/nclimate2145

Uckan, Y., Ruiz-Vásquez, M., De Polt, K., & Orth, R. (2025). Global Relevance of Atmospheric and Land Surface Drivers for Hot Temperature Extremes. *Earth System Dynamics, 16,* 869-889. https://doi.org/10.5194/esd-16-869-2025

van der Walt, A. J., & Fitchett, J. M. (2021). Trend Analysis of Cold Extremes in South Africa: 1960-2016. *International Journal of Climatology, 41,* 2060-2081. https://doi.org/10.1002/joc.6947

Yin, H., & Sun, Y. (2018). Characteristics of Extreme Temperature and Precipitation in China in 2017 Based on ETCCDI Indices. *Advances in Climate Change Research, 9,* 218-226. https://doi.org/10.1016/j.accre.2019.01.001

Zhang, X., Alexander, L., Hegerl, G. C., Jones, P., Tank, A. K., Peterson, T. C. et al. (2011). Indices for Monitoring Changes in Extremes Based on Daily Temperature and Precipitation Data. *WIREs Climate Change, 2,* 851-870. https://doi.org/10.1002/wcc.147